HHS Public Access

Author manuscript

Eur Cell Mater. Author manuscript; available in PMC 2018 August 24.

Published in final edited form as:

Eur Cell Mater. ; 34: 70–82. doi:10.22203/eCM.v034a05.

Cartilage Matrix Remodeling Differs by Disease State and Joint Type

Ming-Feng Hsueh[1], **Virginia Byers Kraus**[1,2], and **Patrik Önnerfjord**[3]

[1]Duke Molecular Physiology Institute, Duke University School of Medicine, Duke University, Durham, NC 27701

[2]Department of Medicine, Duke University School of Medicine, Duke University, Durham, NC 27701

[3]Department of Clinical Sciences Lund, Section of Rheumatology and Molecular Skeletal Biology Center of Excellence in Biological and Medical Mass Spectrometry, Lund University, Lund, Sweden

Abstract

Dramatic alterations in mechanical properties have been documented for osteoarthritic (OA) cartilage. However the matrix composition underlying these changes has not been mapped and their etiology is not entirely understood. We hypothesized that an understanding of the cartilage matrix heterogeneity could provide insights into the origin of these OA-related alterations. We generated serial transverse cryosections for 7 different cartilage conditions: 2 joint sites (knee and hip), 2 disease states (healthy and OA) and 3 tissue depths (superficial, middle, and deep). By laser capture microscopy, we acquired ~200 cartilage matrix specimens from territorial (T) and interterritorial (IT) regions for all 7 conditions; a standardized matrix area was collected for each condition totaling 0.02±0.001 mm^3 (corresponding to 20 μg tissue) from a total of 4800 specimens. Extracted proteins were analyzed for abundance by targeted proteomics.

For most of proteins, a lower IT/T ratio was observed for disease state (OA) and joint type (knee). A major cause of the altered IT/T ratios was decreased protein abundance in IT regions. The collagenase derived type III collagen neo-epitope, indicative of collagen proteolysis, was significantly more abundant in OA cartilage. In addition, it was enriched a mean 1.45 fold in IT relative to T matrix.

These results are consistent with a dominant net proteolysis in IT regions in OA due to degenerative influences, originating from synovial tissue and/or produced locally by chondrocytes. These results provide direct evidence for dynamic remodeling of cartilage and provide a cogent biochemical template for understanding the alterations of matrix mechanical properties.

Correspondence can be sent to: Ming-Feng Hsueh, PhD, Box 104775, Duke Molecular Physiology Institute, Duke University School of Medicine, Durham, NC, 27701, Tel.: 919-681-2004; fax: 919-684-8907. mh167@duke.edu.

Author contributions

M-FH, VBK and PÖ were involved in the conception and design of the study as well as the interpretation of the data. MF-H and PÖ conducted the mass spectrometry experimental work. MF-H conducted the analysis and drafted the manuscript. All authors critically revised the article and gave final approval of the article.

Competing interest statement

The authors have no conflict of interest of any kind with regard to this work.

Keywords

Cartilage Extracellular matrix; Targeted proteomics; i*n situ* trypsin digestion; Laser Capture Microdissection; Territorial Matrix; Interterritorial Matrix

Introduction

Articular cartilage is a highly organized tissue with a low-friction surface that acts to facilitate joint mobility; its tightly integrated structure withstands high mechanical load during movement (Bhosale and Richardson, 2008; Buckwalter and Mankin, 1998; Teeple *et al.*, 2008). The articular cartilage above the tidemark can be separated into three distinct layers (superficial, middle, and deep layers) differing by histological characteristics, specifically, morphology and density of chondrocytes, collagen type, diameter, orientation, and matrix protein composition (Buckwalter *et al.*, 2005). The structural organization of articular cartilage also differs regionally by the distance of the matrix from chondrocytes (pericellular, territorial and interterritorial) (Bhosale and Richardson, 2008; Buckwalter and Mankin, 1998; Guilak *et al.*, 2006). Moreover, until recently, it was not realized that articular cartilage from different joint sites differ quite significantly in many of their protein constituents (Önnerfjord *et al.*, 2012); these differences may have evolved in response to differences in the tissue mechanical environments or arisen secondarily, as a result of joint pathology.

Past studies evaluating the protein content of cartilage by depth have focused on only one or two cartilage components (DiCesare *et al.*, 1995; Lorenzo *et al.*, 1998; Pfister *et al.*, 2001) or used laser capture microdissection (LCM) to evaluate regional differences in gene expression (Fukui *et al.*, 2008a; Fukui et al., 2008b; Landis *et al.*, 2003; Lui *et al.*, 2015) but not protein. A comprehensive evaluation of the subregional differences of articular cartilage has not been performed and this may, in part, be due to the difficulties in distinctly separating subregions of cartilage tissue due to its stiffness and regional complexity. Dramatic alterations in mechanical properties have been documented for osteoarthritic (OA) cartilage (Wilusz *et al.*, 2013) however, the protein matrix architecture underlying these changes has not been mapped and their etiology is not entirely understood. We hypothesized that an understanding of the cartilage protein matrix architecture by joint site, depth and disease state could provide insights into the origin of these OA-related alterations, Moreover, an understanding of human cartilage protein composition heterogeneity across layers, subregions, and joint type is important for elucidating the mechanisms of cartilage homeostasis and pathogenesis of OA in general. This information is also critical for recapitulation of native zonal architecture by tissue-engineering approaches. Our major goal was to gain a comprehensive understanding of the protein network and composition of articular cartilage. Combining separation techniques that included transverse sectioning and LCM, we undertook a decisive phenotyping of cartilage heterogeneity by region, joint type and disease state to gain an understanding of the location of sites with highest protein turnover.

Material and Methods

Clinical cartilage specimen sources

Under Duke Institutional Review Board approval, all articular cartilages were collected from Duke University Hospital as waste surgical specimens. Full thickness cartilage specimens from perilesional regions of the load-bearing area of hip and knee joints were obtained from patients with end stage OA who had arthroplasty surgery. Full thickness healthy non-OA cartilage specimens were collected at the time of surgery for acute trauma; the absence of OA was determined by the surgeon and confirmed by macroscopic inspection upon acquisition of the sample in the laboratory. All specimens were snap frozen, by directly inserting tubes into dry ice, and stored at −80°C.

Cartilage dissection and laser capture microdissection

The sample preparation and workflow are illustrated in Figure 1a. Cartilage specimens were embedded in Tissue-Tek O.C.T. (Sakura, Alphen aan den Rijn, The Netherlands) for cryosectioning. The entire cartilage was sectioned transversely (12μm thick sections) starting from the cartilage surface and progressing to the deep zone. Tissue sections were mounted onto slides covered with polyethylene naphthalate (PEN)-membrane (ZEISS, Oberkochen, Germany) for LCM. Twenty adjacent sections were collected at different distances from the surface to represent the superficial (0–240 μm), middle (480–720 μm), and deep (960–1200 μm) layers. Twenty sections between each layer were skipped to avoid cross-contamination. Decellularization was performed as previously described to remove chondrocyte intracellular proteins from the cartilage extracellular matrix proteome (Hsueh *et al.*, 2016). This step also resulted in the removal of the aqueous embedding media that can adversely affect the liquid chromatography step. Fixation was performed by dropping ice-cold 70% ethanol onto the frozen sections for 5 seconds. For LCM, we obtained approximately 200 laser microdissected specimens from 10 sections for each distinct subregion (interterritorial and territorial matrix) at each cartilage depth (superficial, middle and deep) and derived from healthy and OA knees and hips. A total of 24 groups of sections, including 3 depths, 2 types of joints, 2 types of disease status and 2 types of subregions, were derived from the following subjects: a 56 year old female patient who had knee arthroplasty surgery; a 64 years old female patient who had hip arthroplasty surgery with end stage OA; a 48 year old female patient who had acute knee trauma surgery; and a 35 year old male patient who had acute hip trauma surgery. In total, 4800 specimens were acquired by microdissection representing each joint site, region, depth and disease state. To distinguish the subregions of cartilage for purposes of laser microdissection, tissue sections were stained with toluidine blue dye for 1 min. Sections were dehydrated through exposure to increasing concentrations of ethanol (70%, 95% to 100%). Laser capture microdissection using a Zeiss PALM microbeam system (Zeiss, Oberkochen, Germany) provided the means to collect cartilage matrix from the territorial and interterritorial regions; these regions were distinguished by histological staining characteristics (Henrikson, 1997), i.e. an abrupt decline in toluidine blue staining demarcating the shift from territorial to interterritorial regions. The abrupt transition from dark to light toluidine blue occurred on average 27.4 ±9.6 μm from the cell void; this landmark was distinct in both healthy and osteoarthritic cartilage. The captured subregions of matrix were collected by the wet collection method. In

brief, ammonium bicarbonate (AmBic, Sigma-Aldrich, St. Louis, USA) buffer was added to the cap of a 600 µl microfuge tube that was held in place above the sections. The subregion samples were catapulted from the slide and captured by the wet inner surface of the cap. The same approximate volume of extracellular matrix (0.02±0.001 mm^3 yielding approximately 20 µg tissue) was collected for each specimen.

Specimen preparation for mass spectrometry analysis

By a quick spin of the microfuge tubes, groups of 200 LCM-harvested specimens for a particular region were pooled by immersion in 50mM AmBic containing 0.2% RapiGest (Waters Corporation, Milford, MA), 0.1 Unit Streptococcal hyaluronidase (Seikagaku, Tokyo, Japan), 100 mM 6-aminocaproic acid, 1 mM benzamidine, 1mM EDTA, and 5 mM N-ethylmaleimide, pH7 and heated to 37°C for 3 hours. The specimens were further processed by reduction with 4mM DTT at 56°C for 30 minutes and alkylation with 16 mM iodoacetamide at room temperature for 1h in the dark. Trypsin digestion was performed with 2 µg of trypsin gold (Promega, Madison, WI) at 37°C for 16h. The tryptic peptides were subsequently diluted with 0.5M AmBic and filtered through a 30kDa filter (Pall Life Sciences, Port Washington, NY) followed by a reverse-phase C18 column (The Nest group, Southborough, MA) to remove peptides containing polysaccharide chains and residual salt.

Targeted mass spectrometry analysis

Targeted data acquisition using multiple reaction monitoring (MRM) was performed as previously described (Hsueh *et al.*, 2016; Müller *et al.*, 2014). In brief, processed sample aliquots were quantified using a TSQ Vantage triple quadrupole mass spectrometer (Thermo Scientific, Waltham MA). The mass spectrometer was operated with both Q1 and Q3 settings at 0.7 Da resolution. The on-line reverse-phase chromatographic separation was performed on an Easy nano-LC system (Thermo Scientific, Waltham MA) using a linear binary gradient. A standard mixture of tryptic peptides was run between the samples to check the system performance. The monitored peptide sequence, transitions, and collision energies for MRM were as described previously (Müller *et al.*, 2014). In the present study, we monitored a total of 45 proteins and obtained reliable (matching transitions and retention times) and detectable signals from 30 proteins.

Data analysis

MRM data were analyzed using the Skyline 2.0 software (MacCoss Lab Software, University of Washington). The peak area of MS2 fragment ions (MS/MS), within the expected retention time of the peak, ensured the identity of the peak as measured by synthetic peptides during optimization; MS2 fragment ions were summed for 3–5 transitions for each peptide for MRM experiments. When more than one peptide was available for a particular protein, the peak area of one peptide across the specimens was standardized and the mean standardized values of the peptides derived from one protein were used to represent the protein abundance (Z score). We calculated a ratio to quantify the relative abundance of protein in the interterritorial/territorial (IT/T) matrices; values were log-transformed to achieve normality. For MRM, we compared the protein abundance across the specimens by relative quantification. Multivariable regression was performed with multiple independent factors (joint site - hip/knee), disease state (healthy/OA), depth (superficial,

middle, deep), subregions (territorial/interterritorial) and age of the cartilage to evaluate their association with the continuous outcome response variable (protein abundance). The model evaluated the predicted response due to each specific factor after controlling for the other four factors. We then conducted the Holm step-down procedure to examine the outcome measures controlling the Familywise Error Rate; the p values from the multivariable regression of all monitored proteins were sorted from low to high and then the lowest p value was tested first with a Bonferroni correction involving all tests, the second test was tested with a Bonferroni correction involving one less test and so on for the remaining tests (Abdi, 2010). Statistical significance of each factor and the overall model were reported at the 95% confidence level ($p < 0.05$). The multivariable analyses were performed using JMP® Pro 11.2 (SAS, Cary, NC). All the graphs were prepared in Microsoft Excel, PowerPoint 2013 or GraphPad Prism 5.

Results

Protein abundance distribution patterns in cartilage

Articular cartilage subregions were isolated using LCM; a representative cartilage section is illustrated in Figure 1b (left panel) along with microdissected samples from the territorial matrix (middle panel) and interterritorial matrix (right panel). The transition from territorial to interterritorial matrix was demarcated by an abrupt change in intensity of toluidine blue staining from dark to light which reflects the difference of sulfated glycosaminoglycans (Henrikson, 1997). The size of the territorial matrix could therefore be estimated by the radial distance of this change in staining intensity from the chondrocyte surface. The average radial extent (outer margin) of the territorial matrix from the cell surface was 26.1 ± 6.2 μm in healthy knee cartilage and was significantly less in OA knee cartilage (19.1 ± 8.8 μm). This landmark was also observed in hip cartilage; the average radial extent of the territorial matrix from the cell surface was 34.4 ± 10.6 and 26.2 ± 5.1 μm in healthy and OA hip cartilage, respectively and again was significantly less in OA cartilage. Overall, the radial extent (on average 30.6 ± 9.4 μm) observed in hip cartilage was greater than that in knee cartilage (on average 23.3 ± 8.1 μm).

Protein abundance by joint site—In contrast to all previous studies (Hsueh *et al.*, 2016; Müller *et al.*, 2014; Önnerfjord et al., 2012), the proteomic results represent protein abundance in uniformly sized cartilage samples (Table 1). Among the 30 proteins we monitored, joint site differences were observed in 19 proteins after controlling for other factors; 12 of them remained significant based on the Holm step-down procedure (Table 1). These proteins include aggrecan core protein (G1 and G2 domains) and cartilage oligomeric matrix protein (COMP)–both were significantly enriched in hip cartilage (Figure 2a). Other proteins enriched in hip cartilage included chondroadherin (CHAD), cartilage intermediate layer proteins 1-2, 2-1, and 2-2 (CILP1-2, CILP 2-1, CILP 2-2), type XI collagen (COBA2), versican core protein (CSPG2), dermatopontin (DERM), fibromodulin (FMOD), hyaluronan and proteoglycan link protein 1 (HPLN1), serine protease HTRA1 (HTRA1), matrilin-3 (MATN3), matrix Gla protein (MGP), biglycan (PGS1) and thrombospondin-1, and -4 (TSP1 and TSP4) (Table 1). In contrast to these proteins, one protein, mimecan (MIME), was significantly enriched in knee cartilage (Figure 2a).

Protein abundance by depth—Based on results of the multivariable analyses, most of the proteins were enriched in the deep layer of cartilage, including CILP2-1, fibrillin-1 (FBN1), MGP, aggrecan core protein subdomain (PGCA-3), PGS1, decorin (PGS2), prolargin (PRELP), Target of Nesh-SH3 protein (TARSH) and TSP1 (Figure 2B); CILP1-2, COMP, DERM, fibronectin (FINC), HTRA1, and aggrecan core protein subdomain (PGCA-1/2) were significant based on the Holm step-down procedure. In contrast to these proteins, MIME was significantly enriched in the superficial layer (Figure 2b).

Protein abundance by disease state—We also investigated cartilage protein composition by disease state. CILP1-2, HTRA1, PGCA-1/2, PGS2, TARSH, and TSP1 were all significantly less abundant within OA than healthy cartilage tissue (Figure 2c). COMP remained significantly less abundant within OA cartilage after the Holm step-down procedure. CHAD, MGP and COBA2 were significantly more abundant in OA cartilage tissue; CHAD and MGP were significant based on the Holm step-down procedure (Table 1).

Proteolytic neoepitope—The collagenase derived type III collagen neo-epitope (COL3-neo, IAGITGAR (949–956)), indicative of proteolytic degradation of cartilage, was significantly more abundant in OA cartilage tissue (Healthy −0.67±0.16; OA 0.67±1.03 (Z score)) (Figure 2c) and was enriched a mean 1.45 fold in IT relative to T matrix. The COL3-neo epitope was also significantly enriched in knee compared to hip cartilage (Knee 0.35±1.20; Hip −0.35±0.63); it achieved significance for joint type and disease state based on the Holm step-down procedure. This neoepitoe was also significantly enriched in deep layers of cartilage (Superficial −0.37±0.72; Middle 0.11±1.13; Deep 0.26±1.11) (Table 1).

Protein abundance by cartilage subregion—Unique to this study, we directly investigated protein abundance by cartilage subregion (territorial and interterritorial regions). CILP1-2, HPLN1, MGP, PGCA-1/2, and PGS2 were significantly more abundant in the interterritorial compared to the territorial region (Figure 2d).

Relative protein abundance of Interterritorial/Territorial regions is primarily related to disease state

To evaluate protein alterations in the horizontal plane from the chondrocyte surface, we evaluated the relative abundance of matrix proteins in the interterritorial versus the matched territorial regions as a ratio (IT/T ratio). The abundance of the aggrecan G1/G2 and G3 domains was illustrative of major differences in IT/T ratios. The G1/G2 domain was enriched in the interterritorial matrix of healthy cartilage but was approximately equally abundant within interritorial and territorial subregions of OA cartilage (Figure 3a). The pattern of abundance of the aggrecan G3 domain was the reverse; G3 was enriched in the territorial matrix of healthy cartilage but in the interterritorial matrix of OA cartilage (Figure 3b). Interestingly, the IT/T ratio of the aggrecan core protein did not differ by joint site (hip versus knee) or cartilage depth.

Multivariable regression analyses were used to take all biological factors into consideration simultaneously to identify the independent or specific associations of the biological factors with the protein alterations (Table 2). Generally, disease state and joint type were the

predominant factors affecting the IT/T ratio for most proteins. The IT/T ratios of only 3 proteins were independently affected by cartilage depth (type IX collagen (CO9A1), FBN1, and PGS1). A reduced IT/T ratio in OA cartilage, as seen for HTRA1 and CILP2-2 (Table 2), may be due to a reduction in protein abundance in the interterritorial matrix or by an increased abundance in the territorial matrix, or a combination of both factors. Direct quantification of protein abundance within these subregions revealed that a decreased protein abundance in interterritorial regions was the major cause of the altered IT/T ratios in OA (Figure 4a).

For some proteins, the IT/T ratio was also affected by joint type (Table 2). For instance, type VI collagen (CO6A3), CO9A1, FBN1, HTRA1, MGP, perlecan (PGBM), PGCA-3 and PGS1 were relatively enriched in the interterritorial compared to the territorial matrix of hip cartilage compared to the interterritorial matrix of knee cartilage (Table 2). Among these proteins, only HTRA1 remained significant based on the Holm step-down procedure. Direct quantification of protein abundance revealed that both CO6A3 and HTRA1 were enriched in hip interterritorial matrix (Figure 4b).

Discussion

Our newly developed methodology to comprehensively map protein abundance within articular cartilage tissue yielded some novel insights related to cartilage and alterations in OA. Unique to this study we used LCM, the only tool for separating the cartilage territorial and interterritorial matrix. To our knowledge, no prior study has investigated protein variation by cartilage subregion using LCM. Because extracellular proteins of both the territorial and interterritorial regions are generated by chondrocytes, it is impossible to identify the bona fide differences in these subregions based on genomic (gene expression) strategies alone that have been relied upon in the past to identify zonal differences (Fukui *et al.*, 2008b; Grogan *et al.*, 2013). We calculated the ratio of protein abundance in the interterritorial relative to the territorial region to evaluate the alteration of protein abundance between these two subregions with respect to joint type, disease state, and cartilage depth. Importantly, the ratio was determined from tissue specimens of equal volumes originating from the same horizontal plane thereby providing a means of direct comparison. Interestingly, the alteration of this ratio was primarily related to disease state and joint type. Namely, for most proteins, a lower absolute protein abundance in the interterritorial regions of OA and hip cartilages was responsible for the disease and joint site related changes to the IT/T ratio. In addition, based on toluidine staining, there was an overall diminution in the size of the territorial matrix (defined by intense staining) in OA, and an accompanying increase in the size of the interterritorial matrix (defined by less intense staining and reflecting proteoglycan depletion). These alterations are clear evidence of matrix protein reorganization due to disease.

Type III collagen molecules with unprocessed N-propeptides are present in the extracellular matrix of adult human and bovine articular cartilages as polymers extensively covalently crosslinked to type II collagen (Wu *et al.*, 2010). By immunohistochemical staining with a monoclonal antibody specific to a conformational epitope in the globular N-propeptide domain (Eyre *et al.*, 2006), type III collagen was predominantly concentrated in the

territorial matrix surrounding individual chondrocytes and chondrocyte clusters, strongly implying biosynthesis and deposition by the chondrocytes themselves (Hosseininia *et al.*, 2016). The degradation neo-epitope of type III collagen was first discovered in cartilage explants and their culture media upon treatment with injurious compression and exogenous cytokines (Wang *et al.*, 2016). Our observation in this study confirmed that this type III collagen neo-epitope was generated *in vivo* in OA cartilage tissue. The cleavage neoepitope site is in a region containing repeats of the motif GXP; the cleavage occurs at the Gly-Ile bond, which is analogous to the ¾ - ¼ cleavage site for type II collagen (Howes *et al.*, 2014; Wang *et al.*, 2016). According to the MEROPS database (Rawlings *et al.*, 2010) and consistent with the literature (Billinghurst *et al.*, 1997; Zhen *et al.*, 2008), this epitope is generated by metallopeptidases (MMP-1,-8,-12 and -13). From our previous published work, MMP-1 and MMP-13 were both identified in these specimens (Hsueh *et al.*, 2016). Therefore, the presence of this peptide indicates regions of high proteolytic activity. The higher collagenase derived type III collagen neo-epitope (COL3-neo) that we observed in OA interterritorial regions could contribute to a loss of ECM mechanical properties in OA cartilage. Our data were remarkably consistent with previous studies that have spatially mapped the *in situ* biomechanical properties of articular cartilage (normal human, porcine and murine) via atomic force microscopy. In healthy cartilage, the elastic modulus of the pericellular matrix (PCM) is significantly lower than that of the ECM (Darling *et al.*, 2010). However, in early OA human articular cartilage, the elastic modulus of both the PCM and ECM was reduced by 30% and 45%, respectively (Wilusz *et al.*, 2013). These results are consistent with our observations that the protein abundance varied in the horizontal plane from the chondrocyte surface, with greater declines further from the chondrocyte surface. Our results, therefore, provide potential insights related to the specific protein alterations responsible for the change in mechanical properties in OA.

Mechanical overload can lead to maladaptive cellular responses and cartilage degradation, in part mediated by mechanosensitive ion channels such as PIEZO 1 and 2 (Lee *et al.*, 2014). Mechanical overload in conjunction with proinflammatory mediators, originating from chondrocytes or the milieu of the joint, such as production by synoviocytes, can activate signaling pathways that release chondrocytes from growth arrest and lead to their production of inflammation-related genes, including nitric oxide synthase-2, cyclooxygenase-2, and cartilage proteases such as MMPs-1, 3, and 13, and ADAMTS-4 and 5 (Goldring *et al.*, 2011). Intriguingly, the altered load on osteoblasts and osteocytes also leads to metalloproteinase production (MMPs-3 and -13) by chondrocytes production mediated by bone production of 14-3-3epsilon (Priam *et al.*, 2013). Increased matrix-degrading proteinases generate protein fragments, which can promote further inflammation and cartilage catabolism contributing to the onset or progression of OA (Goldring, 2012). The collagenase derived type III collagen neo-epitope, indicative of collagen proteolysis, was significantly more abundant in OA cartilage tissue and tended to be enriched in the interterritorial matrix. Moreover, this neoepitope was enriched in the deep layer of cartilage tissue. According to our previous work, metallopeptidases capable of generating this neoepitope (MMP-1) tended to be enriched in the deep layer whereas metalloproteinase inhibitors (TIMP1 and 2) tended to be enriched in the superficial layer (Hsueh *et al.*, 2016). Our current results suggest that excess matrix catabolism dominates within the

interterritorial and deep regions and are consistent with a dominant proteolytic influence originating from local aberrantly loaded chondrocytes and/or bone cells. For instance, matrix catabolism originating from proteases in the synovial fluid or chondrocytes may have a predominant effect on the interterritorial regions to generate more neoepitope. Alternatively, the collagen degradation neoepitope may be preferentially cleared in the territorial region by cell-associated mechanisms. A scenario of increased degradation in OA, combined with insufficient protein synthesis, particularly in the interterritorial region would, as we observed, increase the IT/T ratio of the type III collagen neo-epitope and reduce the IT/T ratio of the majority of the other matrix components as an end-result of matrix proteolysis.

Among the unexpected and noteworthy findings was the fact that type VI collagen (CO6A3) was present in the interterritorial domain of both healthy hip and knee cartilage and equally abundant or even slightly enriched in deep layers. These results are in striking contrast to the data in the literature, generated by antibody-based immunohistochemistry, showing that collagen VI is exclusive to the pericellular and territorial matrix (Guilak *et al.*, 2006; Soder *et al.*, 2002). Of note, these prior immunohistochemistry data were all generated without antigen retrievals, such as hyaluronidase or chondroitinase treatment, to reduce the static hindrance due to a dense matrix which could potentially influence the results. Since CO6A3 is believed to be enriched in the chondrocyte territorial, i.e. pericellular matrix, the higher abundance of CO6A3 in the superficial region has been attributed to the higher cellularity of this region. However, our results are based on proteomic analyses of a standardized volume of cartilage matrix, excluding cells, thereby reflecting absolute abundance in the matrix. We know from our previous study that *in situ* digestion of cartilage yields ~3 fold more type VI collagen than guanidine-HCl extraction suggesting that a large proportion of type VI collagen may be associated with a guanidine-HCl resistant collagen framework (Hsueh *et al.*, 2016). Given that this collagen framework is likely much less accessible to antibody penetration than the proteoglycan component, prior reports of CO6A3 localization seem to have underestimated total CO6A3, instead identifying a more accessible subpopulation of CO6A3 associated with proteoglycans in the superficial layer (Hsueh *et al.*, 2016; Müller *et al.*, 2014).

Many studies have made efforts to understand articular cartilage protein heterogeneity using proteomic methods. Even though the strategies used have been different, the results are consistent. For instance, we observed enrichment of the aggrecan G3 domain in the interterritorial matrix of OA cartilage compared with enrichment in the territorial matrix of healthy cartilage. These observations are consistent with previous studies reporting matrix reorganization; these studies included the existence of different proteoglycan pools within the cartilage (Maroudas *et al.*, 1998), the observation of radiolabeled newly synthesized aggrecan in the territorial regions in control bovine cartilage explant cultures (Handley *et al.*, 2002), and the redistribution of the radiolabeled newly synthesized aggrecan into the interterritorial regions upon exposure to retinoic acid that leads to cartilage degradation (Handley *et al.*, 2002). Our findings that HPLN1 and CHAD were enriched in hip compared to knee cartilage are also consistent with past studies, which showed more than two-fold enrichment in hip compared to knee cartilage (Hsueh *et al.*, 2016; Önnerfjord et al., 2012).

Our finding that mimecan was the only protein demonstrating a significant enrichment in knee cartilage agrees with a past quantitative study showing mimecan to be the most enriched protein in knee cartilage (four-fold more compared to hip cartilage) (Önnerfjord *et al.*, 2012). Mimecan, also known as osteoglycin or osteoinductive factor, belongs to the family of small leucine rich proteoglycans (SLRPs) which are abundant in the bone matrix, cartilage cells, and connective tissues, and are thought to regulate cell proliferation, differentiation and adhesion (Hamajima *et al.*, 2003). Consistent with our observation of enrichment of mimecan in the articular cartilage superficial zone, Zone-specific DNA array analysis demonstrates enrichment of mimecan in superficial compared with deep zones of human and bovine articular cartilage (Grogan *et al.*, 2013).

The LCM system we used consists of a highly-automated microscope platform and a pulsed-UV laser system. The system generated a laser microbeam able to cut cartilage matrix along any desired path with a focal point less than 1 μm diameter. This high-resolution laser (<1 μm) enabled the collection of ultrapure, selected material from heterogeneous regions of interest for downstream applications. Given the high resolution of the laser, this method can be applied to the isolation of cartilage tissue from multiple species, both large and small, including bovine (Landis *et al.*, 2005), human (Fukui *et al.*, 2008a; Fukui et al., 2008b), rat (Mori *et al.*, 2014) and murine (Landis *et al.*, 2003; Yamane *et al.*, 2007) species. However, none of these studies evaluated the subregional differences; rather, all these studies focused on genomic profiling and expression differences by depth within cartilage. In our present study, we demonstrated the feasibility, even with very limited material (0.02 ± 0.001 mm^3), of evaluating the subregional composition of the extracellular matrix by combining LCM and proteomic methodology. This methodology is very applicable to small animal tissues since the laser focal point (<1 μm) is much smaller than the thickness of their cartilage tissue (e.g. 30 μm for mouse distal femoral articular cartilage and 300 μm for guinea pig tibial articular cartilage) (Aigner *et al.*, 2010). However, because these small animal articular cartilages are more hypercellular than human tissue, it is to be expected that more time and cost may be involved in collecting sufficient samples for analysis. This methodology could be applied to analyze the therapeutic efficiency of drugs or cartilage repair strategies in OA animal model systems and thereby, in the long run, advance treatments for human OA.

This study was limited in its approach due to its focus on candidate proteins, albeit a larger number studied than in previously published work, and few patient specimens, although all results were adjusted for specimen age. Among the surprising results provided by the proteomic analysis was the clear evidence of collagen VI protein expression beyond the territorial matrix. Unfortunately, no robust method, such as a well-validated ELISA, was available to confirm these intriguing collagen VI proteomic results. Expanding this paradigmatic investigation to the whole proteome by non-targeted proteomic approaches will be advantageous in future to gain an even more detailed understanding of cartilage compositional changes due to joint site, disease, depth, and subregion.

In this study, we utilized a comprehensive methodology of profiling the composition of cartilage across subregions by combining laser capture microscopy and proteomics. This protocol provides a direct and thorough means of investigating cartilage that overcomes some inherent difficulties of analyzing this matrix rich tissue. Targeting multiple important

matrix proteins provided a paradigm for a holistic investigation of cartilage tissue composition. This study revealed that degradation of the interterritorial region of articular cartilage is one of the main consequences of OA.

Acknowledgments

Role of funding sources

This study was supported by OARSI Collaborative Scholarship to M-FH, Collaborative Exchange Award from the Orthopaedic Research Society to VBK; and NIH/NIA P30-AG-028716. Mass spectrometers were funded by the Crafoord Foundation and Inga-Britt and Arne Lundberg Foundation and other financial support were obtained from the Swedish Research Council (2010-2889) to PÖ.

References

Abdi H. Holm's sequential Bonferroni procedure. Encyclopedia of research design. 2010; 1

Aigner T, Cook JL, Gerwin N, Glasson SS, Laverty S, Little CB, McIlwraith W, Kraus VB. Histopathology atlas of animal model systems - overview of guiding principles. Osteoarthritis Cartilage. 2010; 18(Suppl 3):S2–6. [PubMed: 20864020]

Bhosale AM, Richardson JB. Articular cartilage: structure, injuries and review of management. Br Med Bull. 2008; 87:77–95. [PubMed: 18676397]

Billinghurst RC, Dahlberg L, Ionescu M, Reiner A, Bourne R, Rorabeck C, Mitchell P, Hambor J, Diekmann O, Tschesche H, Chen J, Van Wart H, Poole AR. Enhanced cleavage of type II collagen by collagenases in osteoarthritic articular cartilage. J Clin Invest. 1997; 99:1534–1545. [PubMed: 9119997]

Buckwalter JA, Mankin HJ. Articular cartilage: tissue design and chondrocyte-matrix interactions. Instr Course Lect. 1998; 47:477–486. [PubMed: 9571449]

Buckwalter JA, Mankin HJ, Grodzinsky AJ. Articular cartilage and osteoarthritis. Instr Course Lect. 2005; 54:465–480. [PubMed: 15952258]

Darling EM, Wilusz RE, Bolognesi MP, Zauscher S, Guilak F. Spatial mapping of the biomechanical properties of the pericellular matrix of articular cartilage measured in situ via atomic force microscopy. Biophys J. 2010; 98:2848–2856. [PubMed: 20550897]

DiCesare PE, Morgelin M, Carlson CS, Pasumarti S, Paulsson M. Cartilage oligomeric matrix protein: isolation and characterization from human articular cartilage. J Orthop Res. 1995; 13:422–428. [PubMed: 7602403]

Eyre DR, Weis MA, Wu JJ. Articular cartilage collagen: an irreplaceable framework? Eur Cell Mater. 2006; 12:57–63. [PubMed: 17083085]

Fukui N, Ikeda Y, Ohnuki T, Tanaka N, Hikita A, Mitomi H, Mori T, Juji T, Katsuragawa Y, Yamamoto S, Sawabe M, Yamane S, Suzuki R, Sandell LJ, Ochi T. Regional differences in chondrocyte metabolism in osteoarthritis: a detailed analysis by laser capture microdissection. Arthritis Rheum. 2008a; 58:154–163. [PubMed: 18163492]

Fukui N, Miyamoto Y, Nakajima M, Ikeda Y, Hikita A, Furukawa H, Mitomi H, Tanaka N, Katsuragawa Y, Yamamoto S, Sawabe M, Juji T, Mori T, Suzuki R, Ikegawa S. Zonal gene expression of chondrocytes in osteoarthritic cartilage. Arthritis Rheum. 2008b; 58:3843–3853. [PubMed: 19035477]

Goldring MB. Articular Cartilage Degradation in Osteoarthritis. HSS Journal. 2012; 8:7–9. [PubMed: 23372517]

Goldring MB, Otero M, Plumb DA, Dragomir C, Favero M, El Hachem K, Hashimoto K, Roach HI, Olivotto E, Borzi RM, Marcu KB. Roles of Inflammatory and Anabolic Cytokines in Cartilage Metabolism: Signals and Multiple Effectors Converge Upon Mmp-13 Regulation in Osteoarthritis. European cells & materials. 2011; 21:202–220. [PubMed: 21351054]

Grogan SP, Duffy SF, Pauli C, Koziol JA, Su AI, D'Lima DD, Lotz MK. Zone-specific gene expression patterns in articular cartilage. Arthritis Rheum. 2013; 65:418–428. [PubMed: 23124445]

Guilak F, Alexopoulos LG, Upton ML, Youn I, Choi JB, Cao L, Setton LA, Haider MA. The pericellular matrix as a transducer of biomechanical and biochemical signals in articular cartilage. Ann N Y Acad Sci. 2006; 1068:498–512. [PubMed: 16831947]

Hamajima S, Hiratsuka K, Kiyama-Kishikawa M, Tagawa T, Kawahara M, Ohta M, Sasahara H, Abiko Y. Effect of low-level laser irradiation on osteoglycin gene expression in osteoblasts. Lasers Med Sci. 2003; 18:78–82. [PubMed: 12928816]

Handley CJ, Winter GM, Ilic MZ, Ross JM, Anthony Poole C, Clem Robinson H. Distribution of newly synthesized aggrecan in explant cultures of bovine cartilage treated with retinoic acid. Matrix Biol. 2002; 21:579–592. [PubMed: 12475642]

Henrikson, RC. Histology. Vol. 10. Williams & Wilkins; Baltimore: 1997. p. 122-124.

Hosseininia S, Weis MA, Rai J, Kim L, Funk S, Dahlberg LE, Eyre DR. Evidence for enhanced collagen type III deposition focally in the territorial matrix of osteoarthritic hip articular cartilage. Osteoarthritis and cartilage/OARS, Osteoarthritis Research Society. 2016; 24:1029–1035.

Howes J-M, Bihan D, Slatter DA, Hamaia SW, Packman LC, Knauper V, Visse R, Farndale RW. The Recognition of Collagen and Triple-helical Toolkit Peptides by MMP-13: SEQUENCE SPECIFICITY FOR BINDING AND CLEAVAGE. The Journal of Biological Chemistry. 2014; 289:24091–24101. [PubMed: 25008319]

Hsueh MF, Khabut A, Kjellström S, Önnerfjord P, Kraus VB. Elucidating the Molecular Composition of Cartilage by Proteomics. J Proteome Res. 2016; 15:374–388. [PubMed: 26632656]

Landis WJ, Jacquet R, Hillyer J, Lowder E, Yanke A, Siperko L, Asamura S, Kusuhara H, Enjo M, Chubinskaya S, Potter K, Isogai N. Design and assessment of a tissue-engineered model of human phalanges and a small joint. Orthod Craniofac Res. 2005; 8:303–312. [PubMed: 16238611]

Landis WJ, Jacquet R, Hillyer J, Zhang J. Analysis of osteopontin in mouse growth plate cartilage by application of laser capture microdissection and RT-PCR. Connect Tissue Res. 2003; 44(Suppl 1): 28–32. [PubMed: 12952170]

Lee W, Leddy HA, Chen Y, Lee SH, Zelenski NA, McNulty AL, Wu J, Beicker KN, Coles J, Zauscher S, Grandl J, Sachs F, Guilak F, Liedtke WB. Synergy between Piezo1 and Piezo2 channels confers high-strain mechanosensitivity to articular cartilage. Proc Natl Acad Sci U S A. 2014; 111:E5114–5122. [PubMed: 25385580]

Lorenzo P, Bayliss MT, Heinegård D. A novel cartilage protein (CILP) present in the mid-zone of human articular cartilage increases with age. J Biol Chem. 1998; 273:23463–23468. [PubMed: 9722583]

Lui JC, Chau M, Chen W, Cheung CSF, Hanson J, Rodriguez-Canales J, Nilsson O, Baron J. Spatial regulation of gene expression during growth of articular cartilage in juvenile mice. Pediatr Res. 2015; 77:406–415. [PubMed: 25521919]

Maroudas A, Bayliss MT, Uchitel-Kaushansky N, Schneiderman R, Gilav E. Aggrecan turnover in human articular cartilage: use of aspartic acid racemization as a marker of molecular age. Arch Biochem Biophys. 1998; 350:61–71. [PubMed: 9466821]

Mori Y, Chung UI, Tanaka S, Saito T. Determination of differential gene expression profiles in superficial and deeper zones of mature rat articular cartilage using RNA sequencing of laser microdissected tissue specimens. Biomed Res. 2014; 35:263–270. [PubMed: 25152035]

Müller C, Khabut A, Dudhia J, Reinholt FP, Aspberg A, Heinegård D, Önnerfjord P. Quantitative proteomics at different depths in human articular cartilage reveals unique patterns of protein distribution. Matrix Biol. 2014:34–45.

Önnerfjord P, Khabut A, Reinholt FP, Svensson O, Heinegård D. Quantitative proteomic analysis of eight cartilaginous tissues reveals characteristic differences as well as similarities between subgroups. J Biol Chem. 2012; 287:18913–18924. [PubMed: 22493511]

Pfister BE, Aydelotte MB, Burkhart W, Kuettner KE, Schmid TM. Del1: a new protein in the superficial layer of articular cartilage. Biochem Biophys Res Commun. 2001; 286:268–273. [PubMed: 11500032]

Priam S, Bougault C, Houard X, Gosset M, Salvat C, Berenbaum F, Jacques C. Identification of soluble 14-3-3 as a novel subchondral bone mediator involved in cartilage degradation in osteoarthritis. Arthritis Rheum. 2013; 65:1831–1842. [PubMed: 23552998]

Rawlings ND, Barrett AJ, Bateman A. MEROPS: the peptidase database. Nucleic Acids Research. 2010; 38:D227–D233. [PubMed: 19892822]

Soder S, Hambach L, Lissner R, Kirchner T, Aigner T. Ultrastructural localization of type VI collagen in normal adult and osteoarthritic human articular cartilage. Osteoarthritis Cartilage. 2002; 10:464–470. [PubMed: 12056849]

Teeple E, Elsaid KA, Fleming BC, Jay GD, Aslani K, Crisco JJ, Mechrefe AP. Coefficients of friction, lubricin, and cartilage damage in the anterior cruciate ligament-deficient guinea pig knee. J Orthop Res. 2008; 26:231–237. [PubMed: 17868097]

Wang Y, Li Y, Khabut A, Chubinskaya S, Grodzinsky AJ, Önnerfjord P. Quantitative proteomics analysis of cartilage response to mechanical injury and cytokine treatment. Matrix Biol. 2016

Wilusz RE, Zauscher S, Guilak F. Micromechanical mapping of early osteoarthritic changes in the pericellular matrix of human articular cartilage. Osteoarthritis Cartilage. 2013; 21:1895–1903. [PubMed: 24025318]

Wu JJ, Weis MA, Kim LS, Eyre DR. Type III collagen, a fibril network modifier in articular cartilage. J Biol Chem. 2010; 285:18537–18544. [PubMed: 20404341]

Yamane S, Cheng E, You Z, Reddi AH. Gene expression profiling of mouse articular and growth plate cartilage. Tissue Eng. 2007; 13:2163–2173. [PubMed: 17518732]

Zhen EY, Brittain IJ, Laska DA, Mitchell PG, Sumer EU, Karsdal MA, Duffin KL. Characterization of metalloprotease cleavage products of human articular cartilage. Arthritis Rheum. 2008; 58:2420–2431. [PubMed: 18668564]

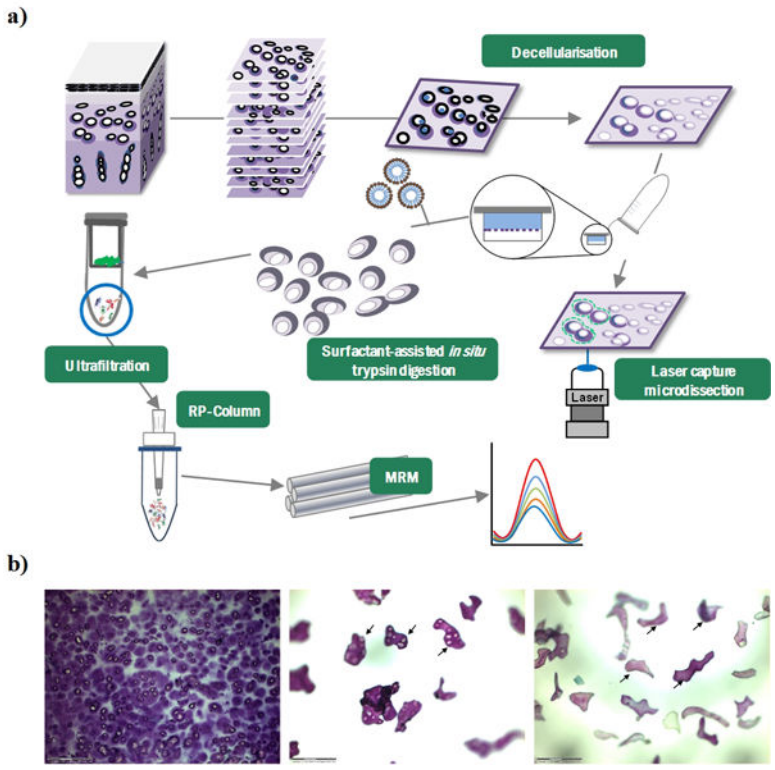

Figure 1. Workflow of laser capture microdissected cartilage tissue proteomic analysis

a) Sections were generated parallel to the articular cartilage surface. Chondrocytes were removed by a previously reported method (Hsueh *et al.*, 2016). Desired subregions were collected separately by laser capture microscopy (LCM). Microdissected samples were collected in the caps of microfuge tubes with AmBic buffer. LCM-harvested sections were treated by *in situ* trypsin digestion method with surfactant as previously described (Hsueh *et al.*, 2016). Extracts were treated by ultrafiltration to remove interfering GAGs and the residual salt was removed by reverse-phase (RP) spin column. Proteomic analyses were performed by LC-triple quadrupole MS (quantitative MRM proteomics). b) The transition from dark to light toluidine blue dye staining marked the regions designated as territorial vs interterritorial, respectively (left). Microscopic examination of (in cap of collection tube) laser captured territorial (middle panel) and interterritorial (right panel) matrix.

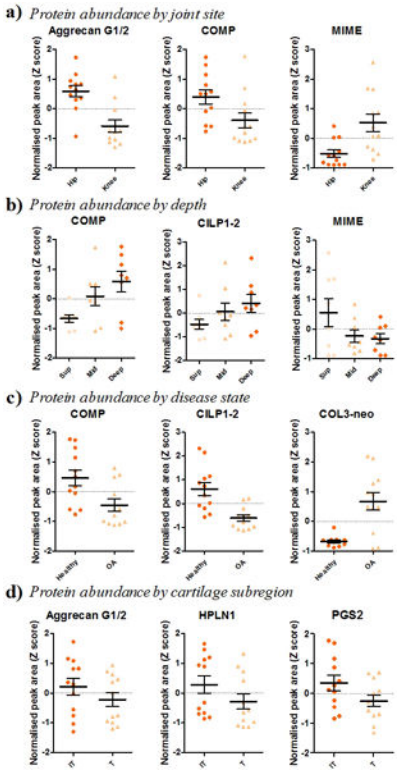

Figure 2. Cartilage matrix protein abundance distribution patterns

Representative proteins demonstrate the a) distribution patterns categorized by joint type, b) distribution patterns categorized by depth of cartilage, c) distribution patterns categorized by disease state, and d) distribution patterns categorized by subregion (interterritorial (IT) vs territorial (T)).

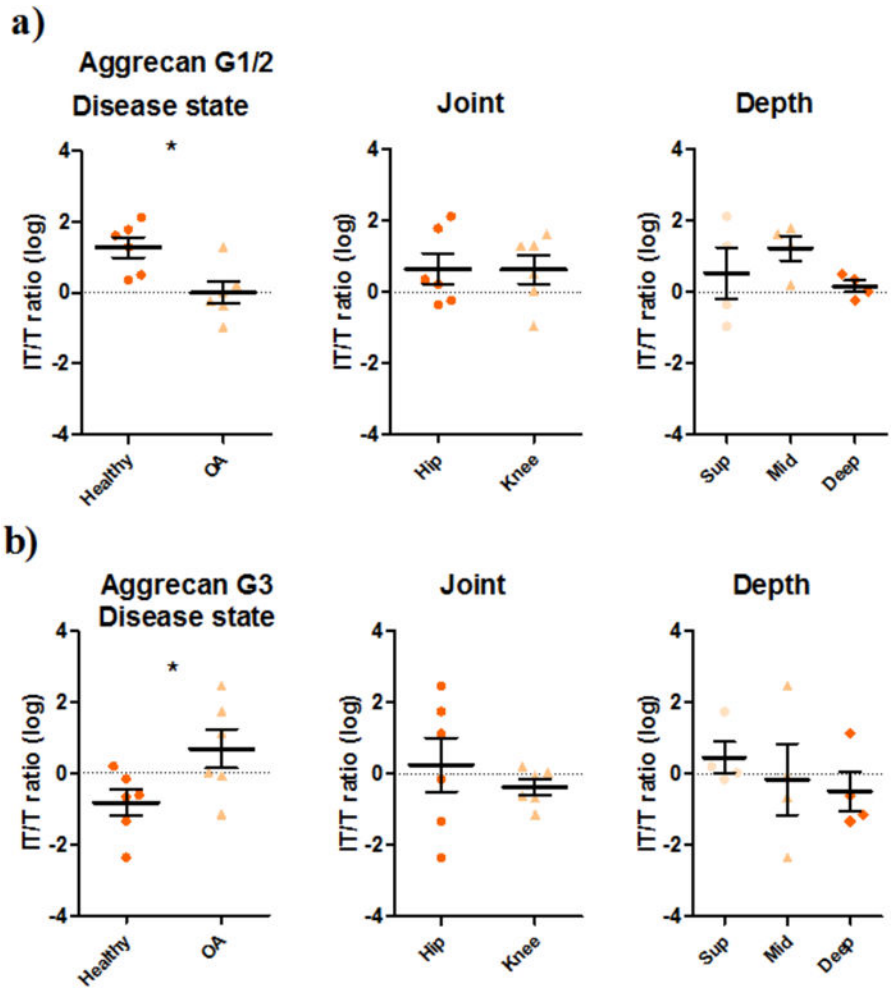

Figure 3. Interterritorial (IT)/Territorial (T) matrix ratio of cartilage matrix proteins

The IT/T ratios of a) aggrecan G1/G2, and (b) G3 proteins categorized by disease state, joint type, and depth of cartilage. The IT/T ratio of aggrecan G1/G2 was significantly higher in healthy cartilage; in a reverse pattern, the ratio of aggrecan G3 was significantly lower in healthy cartilage (P <0.05 by t test). The IT/T ratio of the aggrecan core protein did not differ by joint site (hip versus knee) or cartilage depth. Sup: superficial layer. Mid: middle layer. Deep: deep layer.

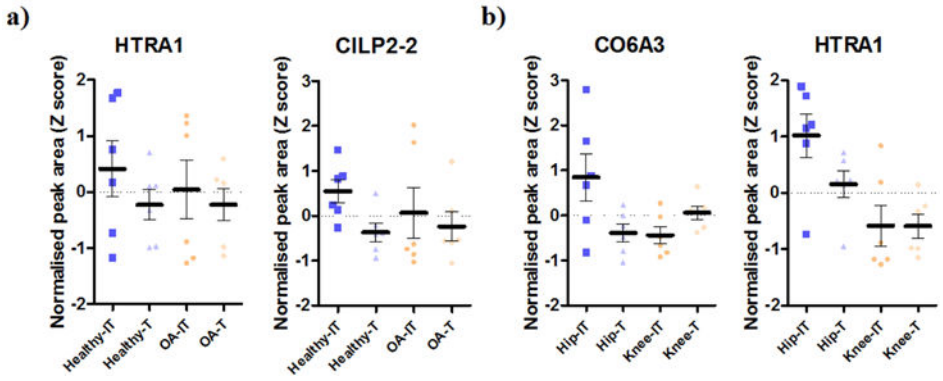

Figure 4. Abundance patterns of proteins with significant IT/T ratio differences by disease state and joint type

Protein abundance distribution categorized by a) disease state, and b) joint type. The abundance of CILP2-2 and HTRA1 proteins within the IT subregion was consistent with a dramatic level of protein degradation or loss in OA. CO6A3 was enriched in the hip interterritorial domain in a different pattern than the knee. HTRA1 was also enriched within the hip interterritorial region.

Table 1

Protein abundance with significant enrichment patterns.

Accession	ID	Protein	*P* value			
			Joint	Disease	Depth	Subregion
O15335	**CHAD**	Chondroadherin	**<.0001**	**<.0001**~	0.4351	0.5551
O75339	**CILP1-1**	Cartilage intermediate layer protein 1 -1	0.0747	0.3249	0.0737	0.2967
O75339	**CILP1-2**	Cartilage intermediate layer protein 1 -2	**<.0001**	**0.0129**	**0.0004**	**0.0295**
Q8IUL8	**CILP2-1**	Cartilage intermediate layer protein 2-1	**0.0003**	0.1404	**0.0304**	0.3735
Q8IUL8	**CILP2-2**	Cartilage intermediate layer protein 2-2	**0.0141**	0.2798	0.2799	0.0728
P02461	**CO3A1**	Collagen alpha-1(III) chain	0.2047	0.8223	0.7824	0.9244
P12111	**CO6A3**	Collagen alpha-3(VI) chain	0.2562	0.8125	0.2558	0.3266
P20849	**CO9A1**	Collagen alpha-1(IX) chain *	0.1493	0.7349	0.0682	0.9254
P13942	**COBA2**	Collagen alpha-2(XI) chain *	**<.0001**	**0.0037**~	0.0545	0.2038
P49747	**COMP**	Cartilage oligomeric matrix protein	**0.0002**	**0.0007**	**<.0001**	0.0643
P13611	**CSPG2**	Versican core protein	**0.0148**	0.6137	0.2340	0.0876
Q07507	**DERM**	Dermatopontin *	**0.0223**	0.5285	**0.0015**	0.2195
P35555	**FBN1**	Fibrillin-1	0.6710	0.8515	**0.0366**	0.1283
P02751	**FINC**	Fibronectin	0.8329	0.6314	**0.0006**	0.3343
Q06828	**FMOD**	Fibromodulin	**0.0150**	0.1035	0.0657	0.0564
P10915	**HPLN1**	Hyaluronan and proteoglycan link protein 1	**<.0001**	0.5130	0.0822	**0.0055**
Q92743	**HTRA1**	Serine protease HTRA1	**<.0001**	**0.0332**	**0.0018**	0.0681
P51884	**LUM**	Lumican *	0.4495	0.4584	0.3424	0.1053
O15232	**MATN3**	Matrilin-3	**0.0009**	0.7281	0.4160	0.5444
P08493	**MGP**	Matrix Gla protein	**<.0001**	**<.0001**~	**0.0049**	**0.0196**
P20774	**MIME**	Mimecan	**0.0052**#	0.4642	**0.0283**^	0.3892
P98160	**PGBM**	Perlecan	0.0703	0.3945	0.1661	0.7221
P16112	**PGCA-1/2**	Aggrecan core protein G1 & G2	**<.0001**	**0.0029**	**0.0010**	**0.0300**
P16112	**PGCA-3**	Aggrecan core protein G3	0.0807	0.4298	**0.0028**	0.7314
P21810	**PGS1**	Biglycan	**0.0075**	0.7316	**0.0040**	0.3318
P07585	**PGS2**	Decorin	0.0840	**0.0360**	**0.0326**	**0.0377**

Accession	ID	Protein	*P* value			
			Joint	Disease	Depth	Subregion
P51888	**PRELP**	Prolargin *	0.1475	0.0941	**0.0025**	0.3946
Q7Z7G0	**TARSH**	Target of Nesh-SH3 *	0.2773	**0.0207**	**0.0120**	0.2719
P07996	**TSP1**	Thrombospondin-1	**0.0007**	**0.0283**	**0.0378**	0.1355
P35443	**TSP4**	Thrombospondin-4	**0.0017**	0.4409	0.3326	0.2062
P02461	**COL3-neo**	Collagen type III neo-epitope	**0.0003**#	**<.0001**~	**0.0139**	0.5999

Table 1 summarizes the results generated from multivariable regression analysis with four independent factors evaluated simutaneously in the models: age, joint site, disease state, cartilage depth, and subregion of cartilage. Text in bold highlights proteins with a *p* value less than 0.05, meaning after controling for the other variables, there was a significant independent association of the protein with either joint site, disease state, depth or subregion. Text with an underlined highlights the proteins with a *p* value less than 0.05 after the Holm step-down procedure.

*Only one peptide was available for a particular protein.

#Mean value was higher in the knee joint.

~Mean value was higher in OA joints.

^Mean value was higher in the superficial layer.

Table 2

Evaluation of IT/T ratio patterns of matrix proteins.

Accession	ID	Protein	Joint			Disease			Depth		
			P value	β	K→ H	P value	β	OA→H	P value	β	S→D
O15335	**CHAD**	Chondroadherin	0.974	0.01	/	0.499	0.46	/	0.827	−0.07	\
O75339	**CILP1-1**	Cartilage intermediate layer protein 1 -1	0.866	0.04	/	0.509	0.35	/	0.214	0.34	/
O75339	**CILP1-2**	Cartilage intermediate layer protein 1 -2	0.529	0.22	/	0.724	0.24	/	0.371	−0.30	\
Q8IUL8	**CILP2-1**	Cartilage intermediate layer protein 2-1	0.918	0.03	/	0.300	0.60	/	0.507	0.18	/
Q8IUL8	**CILP2-2**	Cartilage intermediate layer protein 2-2	0.153	0.36	/	**0.022**	1.29	/	0.119	−0.38	\
P02461	**CO3A1**	Collagen alpha-1(III) chain	0.197	0.40	/	0.508	0.39	\	0.151	−0.44	\
P12111	**CO6A3**	Collagen alpha-3(VI) chain	**0.008**	0.78	/	0.104	0.79	\	0.451	−0.17	\
P20849	**CO9A1**	Collagen alpha-1(IX) chain *	**0.017**	0.49	/	**0.006**	1.20	\	**0.019**	−0.46	\
P13942	**COBA2**	Collagen alpha-2(XI) chain *	0.455	0.24	/	0.134	1.01	/	0.605	0.16	/
P49747	**COMP**	Cartilage oligomeric matrix protein	0.865	0.06	/	0.835	−0.14	/	0.996	0.00	/
P13611	**CSPG2**	Versican core protein	0.944	−0.02	\	0.317	0.63	/	0.401	0.26	/
Q07507	**DERM**	Dermatopontin *	0.294	−0.30	\	0.513	0.36	\	0.064	−0.57	\
P35555	**FBN1**	Fibrillin-1	**<.0001**	0.71	/	**0.002**	0.75	\	**0.015**	−0.24	\
P02751	**FINC**	Fibronectin	0.403	0.30	/	0.679	0.29	/	0.346	0.33	/
Q06828	**FMOD**	Fibromodulin	0.509	−0.14	\	0.111	0.73	/	0.063	−0.43	\
P10915	**HPLN1**	Hyaluronan and proteoglycan link protein 1	0.239	−0.33	\	0.567	0.30	/	0.381	−0.23	\
Q92743	**HTRA1**	Serine protease HTRA1	**0.001**	0.80	/	**0.008**	1.01	/	0.096	0.26	/
P51884	**LUM**	Lumican *	0.430	0.27	/	0.487	0.55	/	0.389	−0.30	\
O15232	**MATN3**	Matrilin-3	0.174	0.50	/	0.465	0.50	/	0.665	−0.14	\
P08493	**MGP**	Matrix Gla protein	**0.016**	0.53	/	**0.005**	1.31	/	0.527	0.11	/
P20774	**MIME**	Mimecan	0.765	−0.08	\	0.078	1.05	/	0.577	0.15	/
P98160	**PGBM**	Perlecan	**0.003**	0.63	/	0.091	0.55	\	0.687	−0.06	\
P16112	**PGCA-1/2**	Aggrecan core protein G1 & G2	0.936	−0.02	/	0.431	0.44	/	0.558	−0.16	\
P16112	**PGCA-3**	Aggrecan core protein G3	**0.035**	0.38	/	0.148	0.47	\	0.074	−0.30	\
P21810	**PGS1**	Biglycan	**0.032**	0.53	/	0.118	0.69	\	**0.022**	−0.56	\
P07585	**PGS2**	Decorin	0.291	0.29	/	0.883	0.08	/	0.469	−0.19	\

Accession	ID	Protein	Joint			Disease			Depth		
			P value	β	K→ H	P value	β	OA→H	P value	β	S→D
P51888	**PRELP**	Prolargin *	0.902	0.04	/	0.322	0.67	/	0.440	−0.25	\
Q7Z7G0	**TARSH**	Target of Nesh-SH3 *	0.903	0.05	/	0.844	−0.15	/	0.468	−0.28	\
P07996	**TSP1**	Thrombospondin-1	0.526	−0.18	\	0.520	0.36	/	0.310	−0.29	\
P35443	**TSP4**	Thrombospondin-4	0.323	0.27	/	**0.033**	1.32	/	0.365	−0.24	\
P02461	**COL3-neo**	Collagen type III neo-epitope	0.320	0.35	/	0.708	0.25	\	0.204	−0.44	\

Table 2 summarize the multivariable model analysis of interterritorial versus territorial (IT/T) ratio of matrix proteins.

*Only one peptide was available for a particular protein. Text in bold highlights proteins with a *p* value less than 0.05, generated from multivariable analysis. Text with an underline highlights the proteins with a *p* value less than 0.05 after the Holm step-down procedure. β=beta coefficients are the estimates resulting from a regression analysis with all variables standardized to a mean of 0 and a variance of 1. K→H: Visualized mean value of knee vs hip cartilage. OA→H: Visualized mean value of OA vs healthy cartilage. S→D: Visualized mean value of superficial vs deep cartilage